



Metallization and Hall-effect of Mg₂Ge under high pressure

Yuqiang Li, Yang Gao, Yonghao Han, Cailong Liu, Gang Peng, Qinglin Wang, Feng Ke, Yanzhang Ma, and Chunxiao Gao

Citation: [Applied Physics Letters](#) **107**, 142103 (2015); doi: 10.1063/1.4932525

View online: <http://dx.doi.org/10.1063/1.4932525>

View Table of Contents: <http://scitation.aip.org/content/aip/journal/apl/107/14?ver=pdfcov>

Published by the [AIP Publishing](#)

Articles you may be interested in

[Effect of temperature and pressure to pinning centers in bulk MgB₂ under high pressure](#)

Low Temp. Phys. **40**, 752 (2014); 10.1063/1.4892647

[Significant enhancement of thermoelectric properties and metallization of Al-doped Mg₂Si under pressure](#)

J. Appl. Phys. **115**, 213705 (2014); 10.1063/1.4881015

[Electronic topological transition and semiconductor-to-metal conversion of Bi₂Te₃ under high pressure](#)

Appl. Phys. Lett. **103**, 052102 (2013); 10.1063/1.4816758

[Raman spectroscopy of ferroelectric Sn₂P₂S₆ under high pressure up to 40 GPa: Phase transitions and metallization](#)

J. Appl. Phys. **113**, 013511 (2013); 10.1063/1.4772624

[Effect of sintering temperature under high pressure on the superconductivity of MgB₂](#)

Appl. Phys. Lett. **78**, 4157 (2001); 10.1063/1.1382632

The logo for AIP APL Photonics is set against a red background with a bright yellow sunburst effect. The letters 'AIP' are in a large, white, sans-serif font, followed by a vertical bar and the words 'APL Photonics' in a smaller, white, sans-serif font.

AIP | APL Photonics

APL Photonics is pleased to announce
Benjamin Eggleton as its Editor-in-Chief



Metallization and Hall-effect of Mg₂Ge under high pressure

Yuqiang Li,^{1,2,3} Yang Gao,^{1,3} Yonghao Han,^{1,a)} Cailong Liu,¹ Gang Peng,¹ Qinglin Wang,^{1,4} Feng Ke,¹ Yanzhang Ma,³ and Chunxiao Gao¹

¹State Key Laboratory of Superhard Materials, Institute of Atomic and Molecular Physics, Jilin University, Changchun 130012, People's Republic of China

²Tianjin Key Laboratory of Advanced Electrical Engineering and Energy Technology, School of Electrical Engineering and Automation, Tianjin Polytechnic University, Tianjin 300387, People's Republic of China

³Department of Mechanical Engineering, Texas Tech University, Lubbock, Texas 79409, USA

⁴Center for High Pressure Science and Technology Advanced Research, Changchun 130012, People's Republic of China

(Received 1 August 2015; accepted 24 September 2015; published online 5 October 2015)

The electrical transport properties of Mg₂Ge under high pressure were studied with the *in situ* temperature-dependent resistivity and Hall-effect measurements. The theoretically predicted metallization of Mg₂Ge was definitely found around 7.4 GPa by the temperature-dependent resistivity measurement. Other two pressure-induced structural phase transitions were also reflected by the measurements. Hall-effect measurement showed that the dominant charge carrier in the metallic Mg₂Ge was hole, indicating the “bad metal” nature of Mg₂Ge. The Hall mobility and charge carrier concentration results pointed out that the electrical transport behavior in the antiferroite phase was controlled by the increase quantity of drifting electrons under high pressure, but in both antiferroite and Ni₂In-type phases it was governed by the Hall mobility. © 2015 AIP Publishing LLC.

[<http://dx.doi.org/10.1063/1.4932525>]

Pressure has always been a good way to endow materials with new and unexpected electrical properties by extremely compressing the distance between atoms. Under high pressures, insulators and semiconductors could become metals, and meanwhile metals could also have possibility to translate into insulators. Both pressure-induced metallization and insulation are important issues in high pressure studies and have been followed with many interests.^{1–5}

Magnesium germanide (Mg₂Ge), due to its superior physical properties of large Seebeck coefficient, low electrical resistivity, and low thermal conductivity,^{6,7} has been considered as a kind of excellent thermoelectric material and motivated intensive studies in the fields of physics, materials science, and chemistry. High pressure physics has also been developing a consuming passion for the properties of Mg₂Ge. Based on the full-potential linearized augmented plane wave method, Mg₂Ge was predicted to go through a pressure-induced metallization at 6.7 GPa.⁸ First-principles calculation showed that Mg₂Ge would experience two first-order structural phase transitions from the initial antiferroite structure to the antiferroite and the Ni₂In-type structures at 8.7 and 33.3 GPa, respectively.⁹ However, most of related studies under high pressure so far still stays at a theoretical level about Mg₂Ge and therefore needs more experiments to give evidence. Besides the pressure-induced metallization and structural phase transitions, furthermore, other important physical parameters, which are useful to understand the electrical transport behavior of Mg₂Ge under high pressures such as Hall coefficient (R_H), carrier concentration (n or p), mobility (μ), and electrical resistivity (ρ), should be also explored.

In this paper, the pressure-induced metallization and the electrical transport properties of Mg₂Ge have been studied by *in situ* temperature-dependent electrical resistivity and Hall-effect measurements under high pressure up to 40 GPa. The possibility of the structural phase transitions in Mg₂Ge was also discussed with the data from the electrical measurements.

The studied object was the Mg₂Ge powder bought from Alfa Aesar Co. with the purity of 99.99%. The initial structure of the sample was checked to be cubic face-centered structure (Space group: Fm-3m, No. 225) by an X-ray diffractometer (XRD) with Cu-K α radiation. Fig. 1(a) shows the XRD spectrum of the initial structure. A nonmagnetic diamond anvil cell (DAC) was utilized to generate high pressure and the anvil culet was 300 μ m in diameter with a bevel angle of 10° for the *in situ* Hall-effect and resistivity measurements. The applied pressure was calibrated by observing the pressure-induced shift of the sharp fluorescent R1 ruby line.^{10,11} A rhenium gasket was preindented to 60 μ m in thickness and then drilled with a hole in diameter of 100 μ m as the sample chamber for the Hall-effect measurement. A T301 stainless steel gasket was used in the temperature-dependent resistivity measurement. The temperature was measured with a standard K-type thermocouple, which was attached to the side face of diamond anvil. No pressure-transmitting medium was used in order to avoid additional error for the electrical parameters measurement, and the sample chamber was fully filled with compacted Mg₂Ge powder. The thickness of the sample under high pressure can be known with an electronic micrometer by measuring the distance between the bottom facets of the two anvils in DAC and then subtracting the total height of the anvils. Relative error has been considered according to previous literature.¹² The deposited molybdenum thin film was patterned into four

^{a)}Author to whom correspondence should be addressed. Email: hanyq@jlu.edu.cn

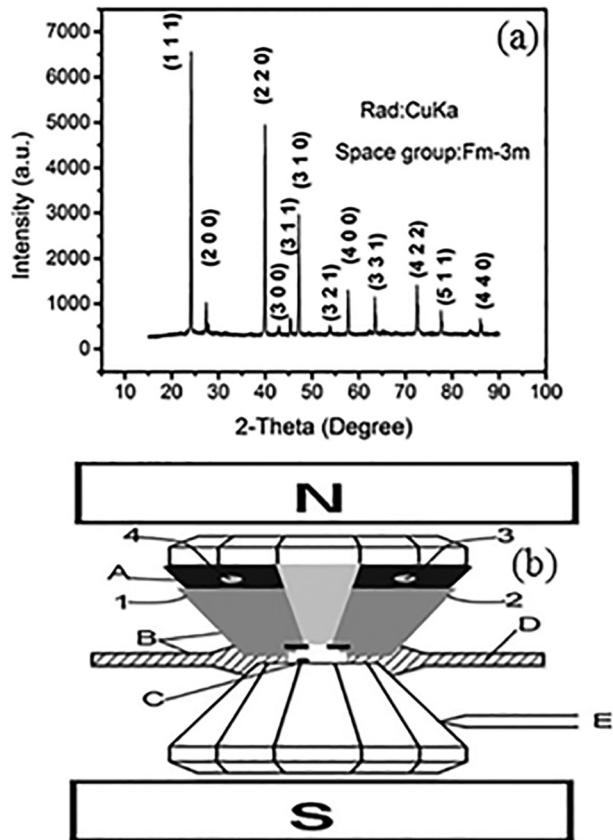


FIG. 1. (a) X-ray diffraction pattern of the Mg_2Ge sample at ambient pressure. (b) The cross sectional view of the designed diamond anvil cell with integrated microcircuit: (A) the Mo electrodes; (B) the Al_2O_3 layer deposited on the Mo film and gasket; (C) the ruby as pressure calibration; (D) the gasket with insulating layer; and (E) the thermocouple; (1), (2), (3), and (4) are the four contact ends of the microcircuit. N and S represent the two poles of magnetic field.

detecting electrodes on one diamond anvil by photolithography technique and chemical etching. The integration process of the microcircuit on the diamond anvil has been reported in previous work.^{13,14} Fig. 1(b) shows the sectional view of the sample configuration with integrated microcircuit in DAC. The electrical resistivity and Hall parameters were determined by van der Pauw equation.^{15,16} The current was detected by a Keithley 2400 source meter, and the voltage was obtained by a Keithley 2700 multimeter. For the Hall-effect measurement, a uniform magnetic field was generated with a maximum value of 20 kG by EM7 electromagnet of East Changing Company and exported through two magnetic heads of 76 mm in diameter. A Lakeshore Gauss meter with model 420 was applied to measure the magnetic field.

The pressure dependence of Mg_2Ge resistivity is shown in Fig. 2. The resistivity decreases with the increasing pressure and three discontinuous changes in resistivity can be found respectively at 7.8, 9.5, and 35.6 GPa, denoting three different pressure-induced transitions (possibly including metallization and structural phase transitions). Theoretical calculations have predicted one metallization at 6.7 GPa (Ref. 8) and two structural phase transitions at 8.7 and 33.3 GPa (Ref. 9) in Mg_2Ge and hereinto it can be seen that the three pressure points of transitions are consistent with the experiment. Comprehensively investigating the theoretical

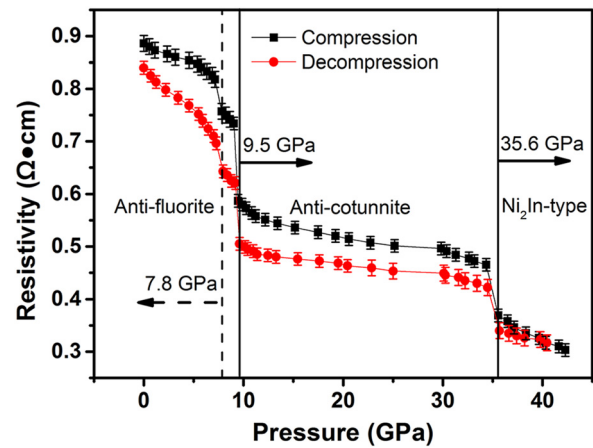


FIG. 2. Pressure dependence of the electrical resistivity of Mg_2Ge at room temperature. Dashed and solid line positions indicate discontinuous pressure. Error bars show the standard deviations resulted from the experiments.

and experimental results and fully considering the possible discrepancy in the two theoretical works, we can definitely know that the third abrupt change in resistivity at 35.6 GPa results from the pressure-induced structural phase transition from the anticotunnite to the Ni_2In -type structure (at 33.3 GPa in theories), but it is still hard to tell apart from the former two transitions which is the metallization and which is the structural phase transition if we just and simply use the resistivity measurement, because the pressure points of metallization and structural phase transition were calculated by two different works and are too close. In order to get a clear transition sequence of Mg_2Ge , successively the temperature-dependent resistivity measurement and Hall-effect measurement have been conducted. Besides, during the decompression, the resistivity can be back to its initial state in a same trend as it did in the process of compression, indicating that the metallization and the structural phase transitions are completely reversible.

Fig. 3 shows the logarithm of resistivity as a function of the reciprocal temperature under various pressures. Rising temperature can activate more charge carriers from

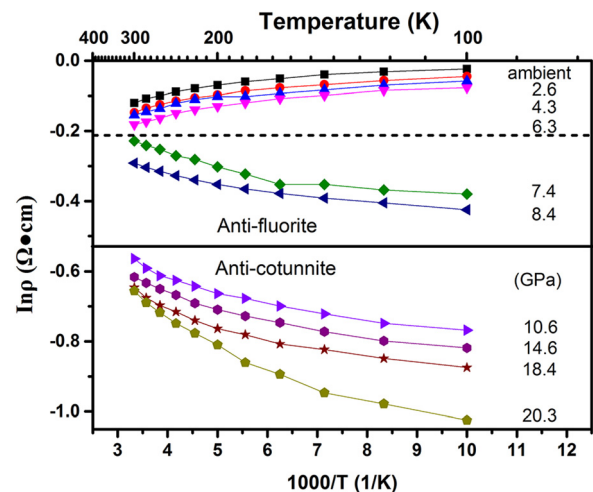


FIG. 3. Reciprocal temperature dependence of the logarithm of resistivity under different pressures. Dashed line position indicates the divider pressure between semiconductor and metallization, and solid line positions represent the pressure of phase transition.

the valence bands (VB) into the conduction bands (CB) in semiconductors, and then the conductivity increases. On the contrary, for metals, rising temperature will enhance the lattice vibrations and increase the possibility of electron scattering by phonons, and then increase the resistivity.^{17,18} Therefore, semiconductor or metallic behavior can be judged by the temperature dependence of resistivity. At pressure less than 7.4 GPa, the resistivity of Mg₂Ge displays a decreasing trend as rising the temperature, which coincides with the electrical conductivity behavior of a semiconductor. While at pressure higher than 7.4 GPa, the resistivity increases with the increasing temperature, indicating that Mg₂Ge has transformed from the semiconductor to a metallic phase. From the temperature-dependent resistivity measurement, we can know that the first transition at around 7.4 to 7.8 GPa should be the metallization of Mg₂Ge, and therefore, the second transition at 9.5 GPa should be the structural phase transition from the antiferroite to the anticotunnite structure.

Hall-effect measurement was conducted for further understanding the electrical properties of Mg₂Ge in a charge-carriers level. In Fig. 4, the abrupt changes of Hall coefficient, Hall mobility, and carrier concentration are shown to be basically consistent with the occurrence of the pressure-induced metallization and structural phase transitions. As the pressure lower than 7.7 GPa, the antiferroite Mg₂Ge remains the n-type semiconducting phase due to the negative Hall coefficients, and the concentration of drifting electrons increases monotonically with the increasing pressure prior to the metallization, proving that the compression can make the conduction band and the valence band widen and the band gap narrow as depicted in the theoretical calculation, and therefore, more electrons can be activated from VB to CB. Although the mobility decreases with the increasing pressure, the increase of electron concentration can still reduce the resistivity.

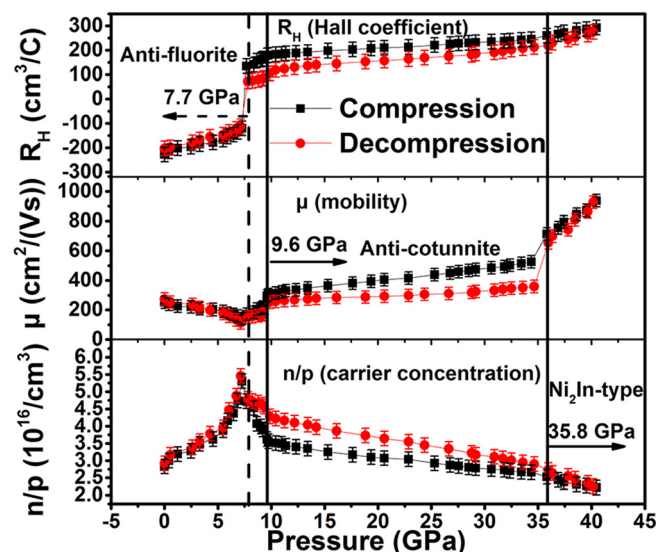


FIG. 4. Pressure dependence of Hall coefficient (R_H), carrier concentration (n or p) and mobility (μ) for Mg₂Ge at room temperature. Dashed line position indicates the pressure of metallization, and solid line positions represent the pressure of phase transition are assigned to three regions. Error bars show the standard deviations resulted from the experiments.

At 7.7 GPa, the metallization occurs. The Hall coefficient switched from negative to positive, indicating that the type of dominant charge carriers in Mg₂Ge changed from electrons to holes. During the transition, the top of VB and the bottom of CB have some overlaps in company with the recombination of some electrons and holes, leading to the decrease of electron carrier concentration, while some electrons will be also tightly bound and cannot move, giving rise to the decrease of the mobility. Electron is the major carrier before the transition, while hole is the major carrier after the transition, the dominance of carrier changes from electron to hole. A detailed description of the crystal structures around phase transitions of Mg₂Ge is useful to understand the n-p transitions. As the antiferroite Mg₂Ge, the Mg²⁺ ions occupy Wyckoff 4(a) sites whereas the Ge⁴⁻ ions are in Wyckoff 8(c) positions. The cell parameter is the only degree of freedom of this structure. The Mg²⁺ ions are coordinated by eight Ge⁴⁻ ions, which are themselves placed at the centers of tetrahedra formed by four Mg²⁺ ions. The coordination ratio is 1:1 between Mg²⁺ and Ge⁴⁻. For the anticotunnite Mg₂Ge (Space group: Pnma, No. 62) after phase transition, all atom occupy Wyckoff 4(c) sites. Hence, this structure has a total of nine degrees of freedom, and each Mg²⁺ ion is surrounded by nine Ge⁴⁻ ions located at the corners of a distorted tricapped trigonal prism. One half of the Ge⁴⁻ ions in the unit cell are coordinated by four Mg²⁺ ions arranged in a slightly distorted tetrahedron. The other half is coordinated by five Mg²⁺ ions arranged in a distorted quadratic pyramid, with three closer-lying cations. The coordination ratio is subtle higher than 1:1 between Mg²⁺ and Ge⁴⁻, therefore the Mg₂Ge shows p type conductive property after phase transition even though the stoichiometric ratios are both 2:1 in two structures.

In general, the metal behavior can be defined as the resistivity increases with the increasing temperature. According to the definition, although Mg₂Ge has presented the metallic transporting behavior under high pressure, the drifting electrons inside would not completely free. The holes can still be the dominant charge carriers to take part in the transporting process, and accordingly the Hall coefficient for the metalized Mg₂Ge is positive. Same phenomena could also be found in Be, Zn, Cd, and some manganese base perovskites.¹⁹⁻²⁵ Hall-effect measurement shows that although the CB and the VB has overlapped at 7.4 GPa, confirmed by theories at 6.7 GPa,⁸ Mg₂Ge is still a “bad metal” after the metallization. Around 7.4 GPa, the Fermi energy levels have intruded into the top of VB (bottom of CB) as the distinguishing feature of degenerate semiconductor, and the quantum states of VB are occupied by holes rather than a small probability condition, in the meantime, the restrictions of Pauli exclusion principle should be considered, which cause the degeneration of carriers leading to the lower carrier concentrations comparing with a true metal.

The Hall coefficient, Hall mobility, and charge carrier concentration of Mg₂Ge also abruptly change at 9.6 and 35.8 GPa, resulting from the two pressure-induced structural phase transitions from the initial antiferroite to the anticotunnite and then to the Ni₂In-type structure, respectively. After 7.7 GPa as shown in Fig. 4, the concentration of holes decreases with the increasing pressure, but the mobility

increases. It indicates that a continuously increased pressure can modify the chemical bonds among atoms and make the quantity of holes to decrease. Meanwhile, the pressure also enhance the rigidity of Mg₂Ge crystal lattice and weaken the hole scattering by the lattice vibration, which make a monotonically increase of the Hall mobility. The combined effect of increased Hall mobility and decreased charge carrier concentration results in the decrease of resistivity in the anticonnute and Ni₂In-type structures of Mg₂Ge under high pressure.

In summary, we carried out the electrical transport properties of Mg₂Ge under high pressure by the *in situ* temperature-dependent resistivity and Hall-effect methods. The temperature-dependent resistivity measurement demonstrated the metallization of Mg₂Ge around 7.4 GPa, which was theoretically predicted, as the pressure can widen the CB and VB bands and narrow the energy band gap in the antiferroite phase resulting in the pressure-induced metallization. Hall-effect measurement showed that hole played a dominant role in the metallic Mg₂Ge as major charge carrier. Resistivity and Hall parameters also reflected the two pressure-induced structural phase transitions by the measurements. The Hall parameters indicated the electrical transport behavior of antiferroite phase was controlled by the increase of drifting electrons quantity under high pressure, while it was governed by the increase of the Hall mobility in both anticonnute and Ni₂In-type phases as pressure modified the chemical bonds among atoms and made the decrease of holes quantity.

This work was supported by the National Basic Research Program of China (Grant No. 2011CB808204), National Natural Science Foundation of China (Grant Nos. 91014004, 11074094, and 11374121), China Postdoctoral Science Foundation (Grant No. 2013M540243), Program of Science and Technology Development Plan of Jilin Province (Grant No. 20140520105JH), and Fundamental

Research Funds for Jilin University, China (Grant No. 450060491500).

- ¹M. P. Pasternak, R. D. Taylor, A. Chen, C. Meade, L. M. Falicov, A. Giesekus, R. Jeanloz, and P. Y. Yu, *Phys. Rev. Lett.* **65**, 790 (1990).
- ²V. A. Sidorov, V. V. Brazhkin, L. G. Khvostantsev, A. G. Lyapin, A. V. Sapelkin, and O. B. Tsiok, *Phys. Rev. Lett.* **73**, 3262 (1994).
- ³R. E. Cohen, I. I. Mazin, and D. G. Isaak, *Science* **275**, 654 (1997).
- ⁴E. Arcangeletti, L. Baldassarre, D. Di Castro, S. Lupi, L. Malavasi, C. Marini, A. Perucchi, and P. Postorino, *Phys. Rev. Lett.* **98**, 196406 (2007).
- ⁵R. S. McWilliams, D. K. Spaulding, J. H. Eggert, P. M. Celliers, D. G. Hicks, R. F. Smith, G. W. Collins, and R. Jeanloz, *Science* **338**, 1330 (2012).
- ⁶J. Tani and H. Kido, *Physica B* **364**, 218 (2005).
- ⁷J. Tani and H. Kido, *Comput. Mater. Sci.* **42**, 531 (2008).
- ⁸F. Kalarasse and B. Benecer, *J. Phys. Chem. Solids* **69**, 1775 (2008).
- ⁹F. Yu, J. Sun, and T. Chen, *Physica B* **406**, 1789 (2011).
- ¹⁰G. J. Piermarini, S. Block, J. D. Barnett, and R. A. Forman, *J. Appl. Phys.* **46**, 2774 (1975).
- ¹¹H. K. Mao, J. Xu, and P. M. Bell, *J. Geophys. Res: Solid Earth.* **91**, 4673 (1986).
- ¹²M. Li, C. Gao, G. Peng, C. He, A. Hao, X. Huang, D. Zhang, C. Yu, Y. Ma, and G. Zou, *Rev. Sci. Instrum.* **78**, 075106 (2007).
- ¹³Y. Han, C. Gao, Y. Ma, H. Liu, Y. Pan, J. Luo, M. Li, C. He, X. Huang, G. Zou, Y. Li, X. Li, and J. Liu, *Appl. Phys. Lett.* **86**, 064104 (2005).
- ¹⁴M. Li, C. Gao, Y. Ma, D. Wang, Y. Li, and J. Liu, *Appl. Phys. Lett.* **90**, 113507 (2007).
- ¹⁵P. M. Hemenger, *Rev. Sci. Instrum.* **44**, 698 (1973).
- ¹⁶Y. Li, Y. Gao, Y. Han, Q. Wang, Y. Li, N. Su, J. Zhang, C. Liu, Y. Ma, and C. Gao, *J. Phys. Chem. C* **116**, 5209 (2012).
- ¹⁷M. I. Eremets, K. Shimizu, T. C. Kobayashi, and K. Amaya, *Science* **281**, 1333 (1998).
- ¹⁸H. Cui, J. S. Brooks, A. Kobayashi, and H. Kobayashi, *J. Am. Chem. Soc.* **131**, 6358 (2009).
- ¹⁹S. Fujita, S. Bedair, M. Littlejohn, and J. Hauser, *J. Appl. Phys.* **51**, 5438 (1980).
- ²⁰W. V. McLevige, K. V. Vaidyanathan, B. G. Streetman, M. Ilegems, J. Comas, and L. Plew, *Appl. Phys. Lett.* **33**, 127 (1978).
- ²¹J. A. Hutchby and K. V. Vaidyanathan, *J. Appl. Phys.* **48**, 2559 (1977).
- ²²H. C. Casey, Jr., F. Ermanis, and K. B. Wolfstirn, *J. Appl. Phys.* **40**, 2945 (1969).
- ²³I. Umebu and P. N. Robson, *J. Cryst. Growth* **53**, 292 (1981).
- ²⁴P. N. J. Dennis, C. T. Elliott, and C. L. Jones, *Infrared Phys.* **22**, 167 (1982).
- ²⁵Y. Shimakawa, Y. Kubo, and T. Manako, *Nature* **379**, 53 (1996).